# Electronic Supplementary Information

## Additional experimental details

*Matrix optimization*

We optimized the solvent composition for the 9-aminoacridine matrix cocktail, so as to obtain a bed of small and homogeneous crystals (**Fig. S-9**). When using 100% acetone, 9-aminoacridine powder dissolved readily, and very small crystals were obtained. However, the matrix aggregated in dense lumps. If water was used to slow the crystallization down, a strong dependence of the crystal size and the water content was observed. With an 8:2 (v/v) mixture of acetone and water, some of the crystals were larger than 20 µm. With a 9:1 (v/v) mixture of acetone and water, the crystal bed was homogeneous with fine crystals being present all around the MAMS spot. The concentration of 9-aminoacridine (2 mg $mL^{-1}$) was also optimized to prevent clogging of the delivery capillary yet to obtain a dense crystal bed.

*Appearance of an algal cell before and after the MALDI process*

We found that the cell is not totally ablated in the MALDI process, which is in contrast to previous studies that were conducted using LDI (without matrix).[1] It must be noted that the laser energy was considerably higher for the LDI measurement ($1.1 \times 10^9$ W $cm^{-2}$ vs. $2.0 \times 10^8$ W $cm^{-2}$ for MALDI of a Nd:YAG laser at a wavelength of 355 nm and a spot size of 40 µm).The cell seems intact and very similar to prior to the matrix application (**Fig. S-10**). This leads us to believe that the matrix is depleted long before the biological material is depleted.

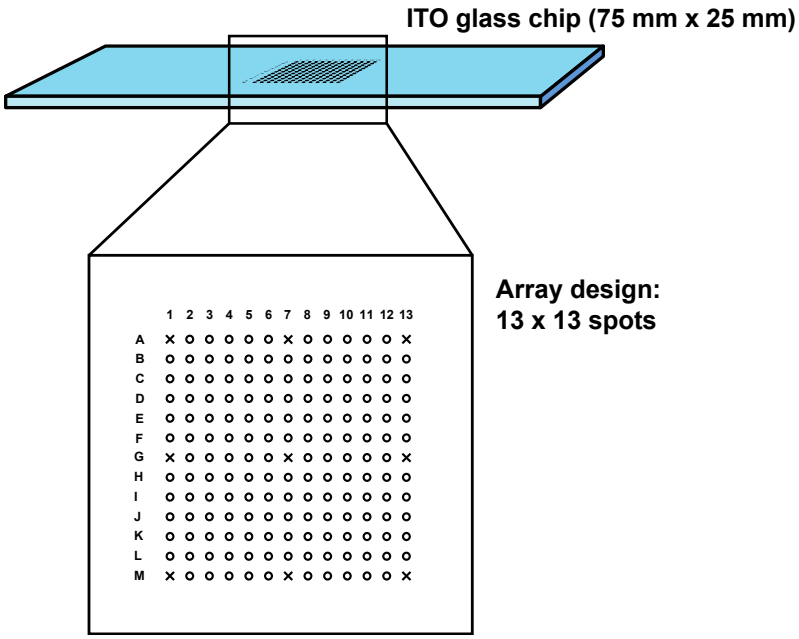


Fig. S-1: Layout of the hydrophilic spots on a MAMS chi[. The circular spots are 100 µm in diameter with a center-to-center spacing of 400 µm. The crosses at the edges and in the center of the chip are used for aligning the chip in the MALDI instrument.

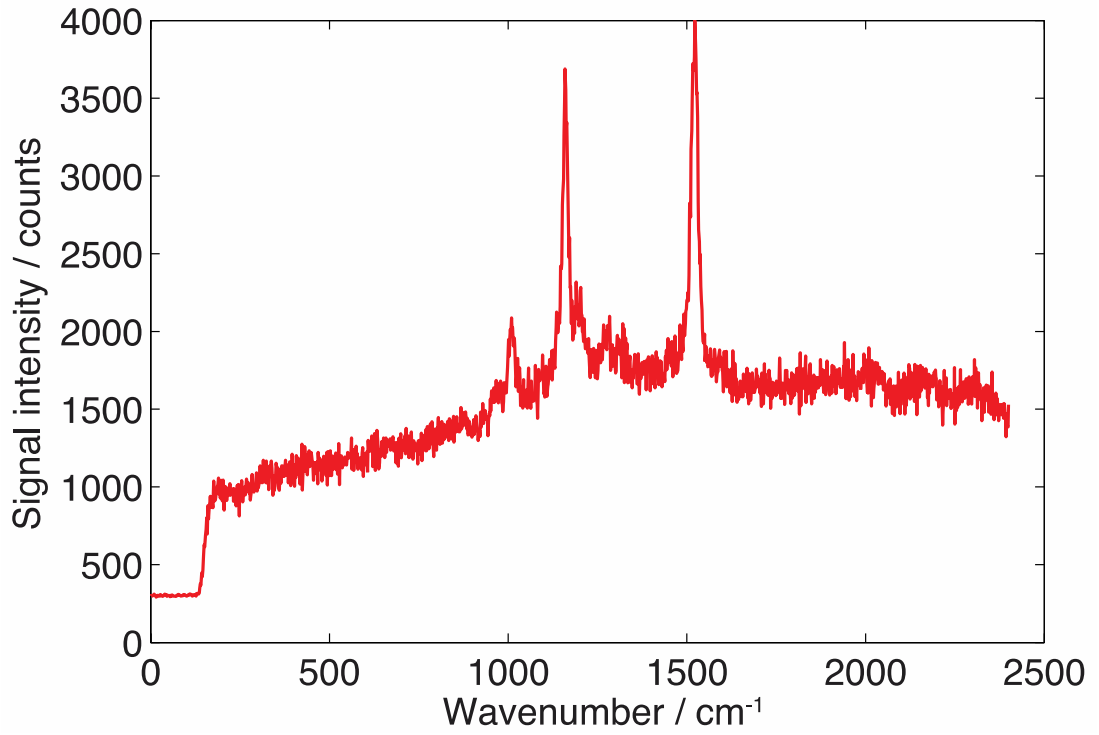


**Fig. S-2** Raman spectrum of the cell in **Fig. 2**.

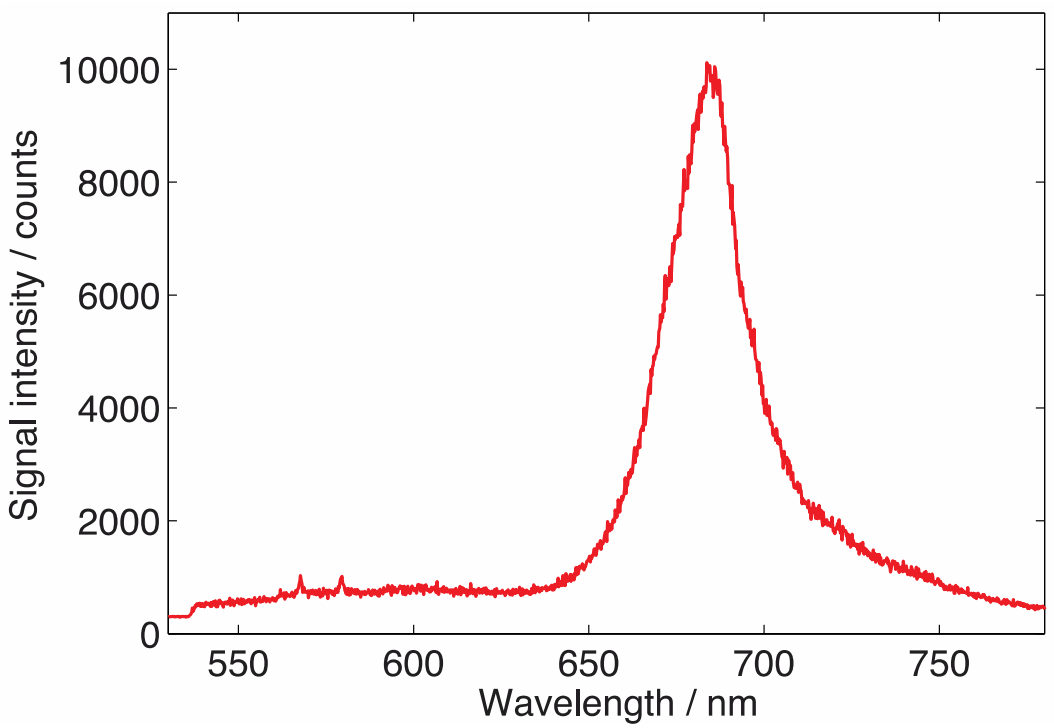


**Fig. S-3** Fluorescence spectrum of the cell shown in **Fig. 2**.

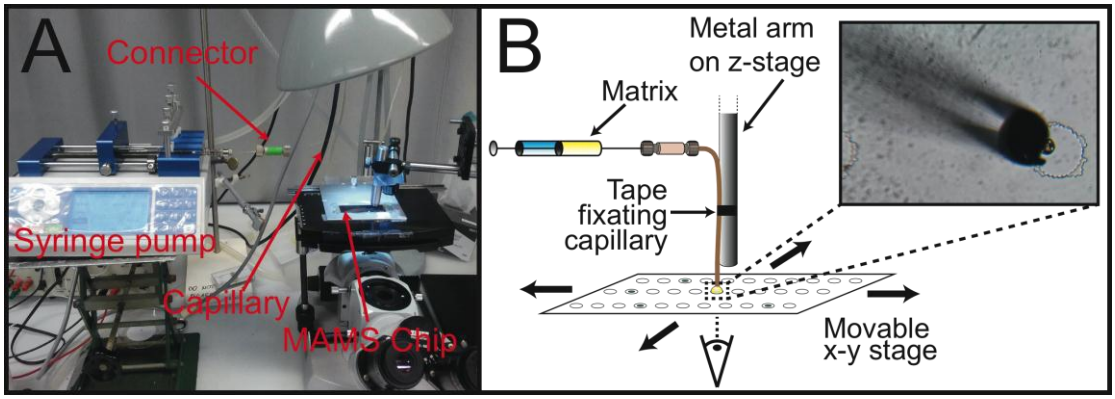


**Fig. S-4** Image (A) and scheme (B) of our system for the deposition of MALDI matrix on microarrays.

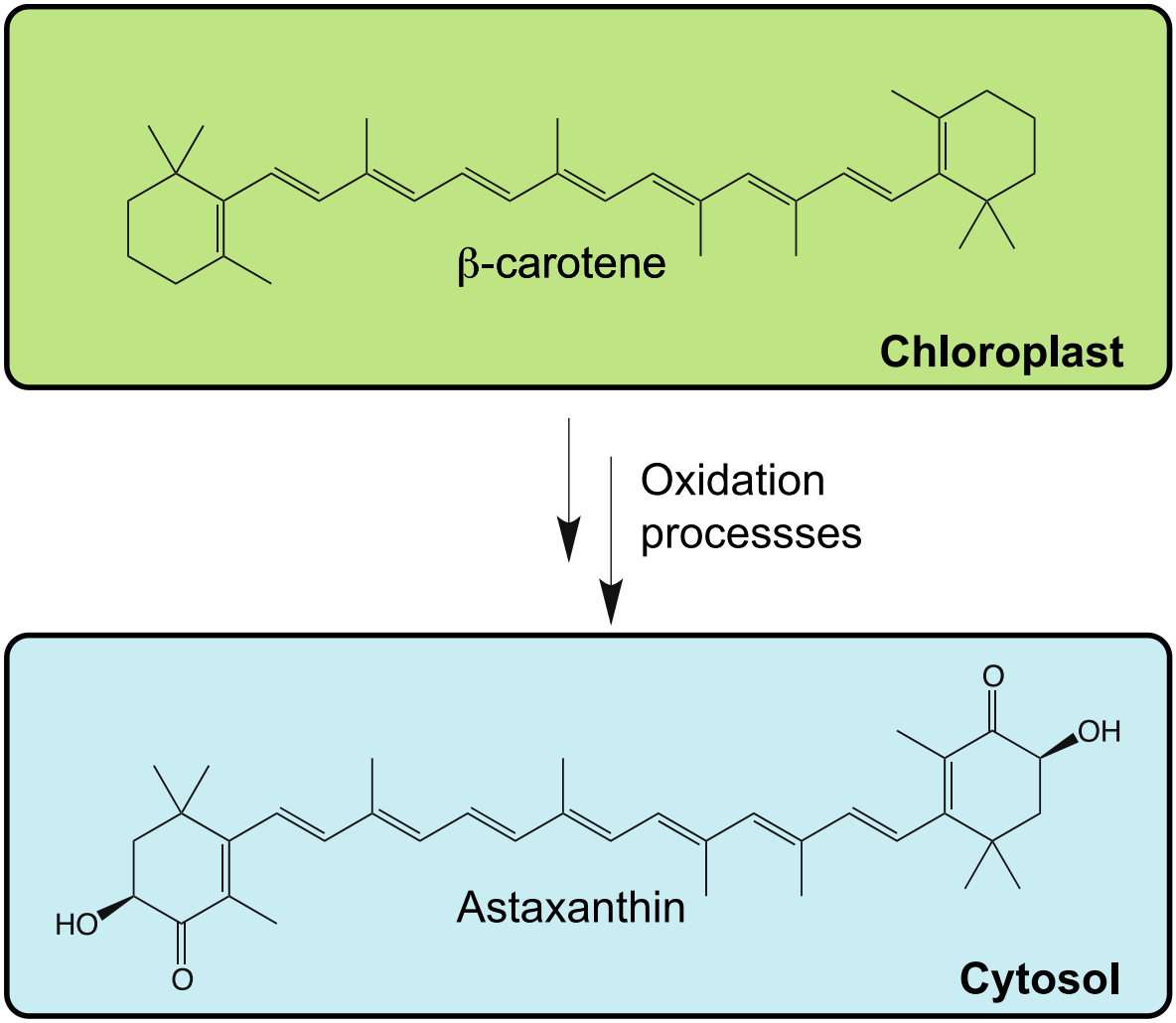


**Fig. S-5** Structure of β-carotene and its derivative astaxanthin, and the location of their biosynthesis.

**Tab. S-1** List of detected metabolites in single *H. pluvialis* cells. The putative assignment is based on the theoretical mass (METLIN database, The Scripps Research Institute, http://www.metlin.scripps.edu). The table contains a list of the detected deprotonated molecules along with theoretical masses of the putative compounds.

| **Metabolite** | **Measured $[M-H]^-$** ***m/z*** | **Theoretical $[M-H]^-$** ***m/z*** |
|---|---|---|
| Phosphoenol pyruvate ($C_3H_4O_6P$) | 166.975 | 166.975 |
| Citrate ($C_6H_7O_7$) | 191.029 | 191.020 |
| Fructose-1,6-bisphosphate ($C_6H_{13}O_{12}P_2$) | 338.981 | 338.989 |
| Adenosine monophosphate ($C_{10}H_{13}N_5O_7P$) | 346.053 | 346.056 |
| Adenosine diphosphate ($C_{10}H_{14}N_5O_{11}P_2$) | 426.023 | 426.022 |
| Uridine triphosphate ($C_9H_{14}N_2O_{15}P_3$) | 482.955 | 482.961 |
| Adenosine triphosphate ($C_{10}H_{15}N_5O_{13}P_3$) | 505.992 | 505.989 |
| Guanosine triphosphate ($C_{10}H_{15}N_5O_{14}P_3$) | 521.961 | 521.983 |
| Uridine diphosphate pentose ($C_{14}H_{21}N_2O_{16}P_2$) | 535.030 | 535.037 |
| Uridine diphosphate hexose ($C_{15}H_{23}N_2O_{17}P_2$) | 565.044 | 565.045 |
| Sulfoquinovose diacylglycerol ($C_{41}H_{77}O_{12}S$, 32:0) | 793.530 | 793.516 |
| Sulfoquinovose diacylglycerol ($C_{43}H_{75}O_{12}S$, 34:3) | 815.530 | 815.498 |
| Sulfoquinovose diacylglycerol ($C_{43}H_{77}O_{12}S$, 34:2) | 817.533 | 817.514 |

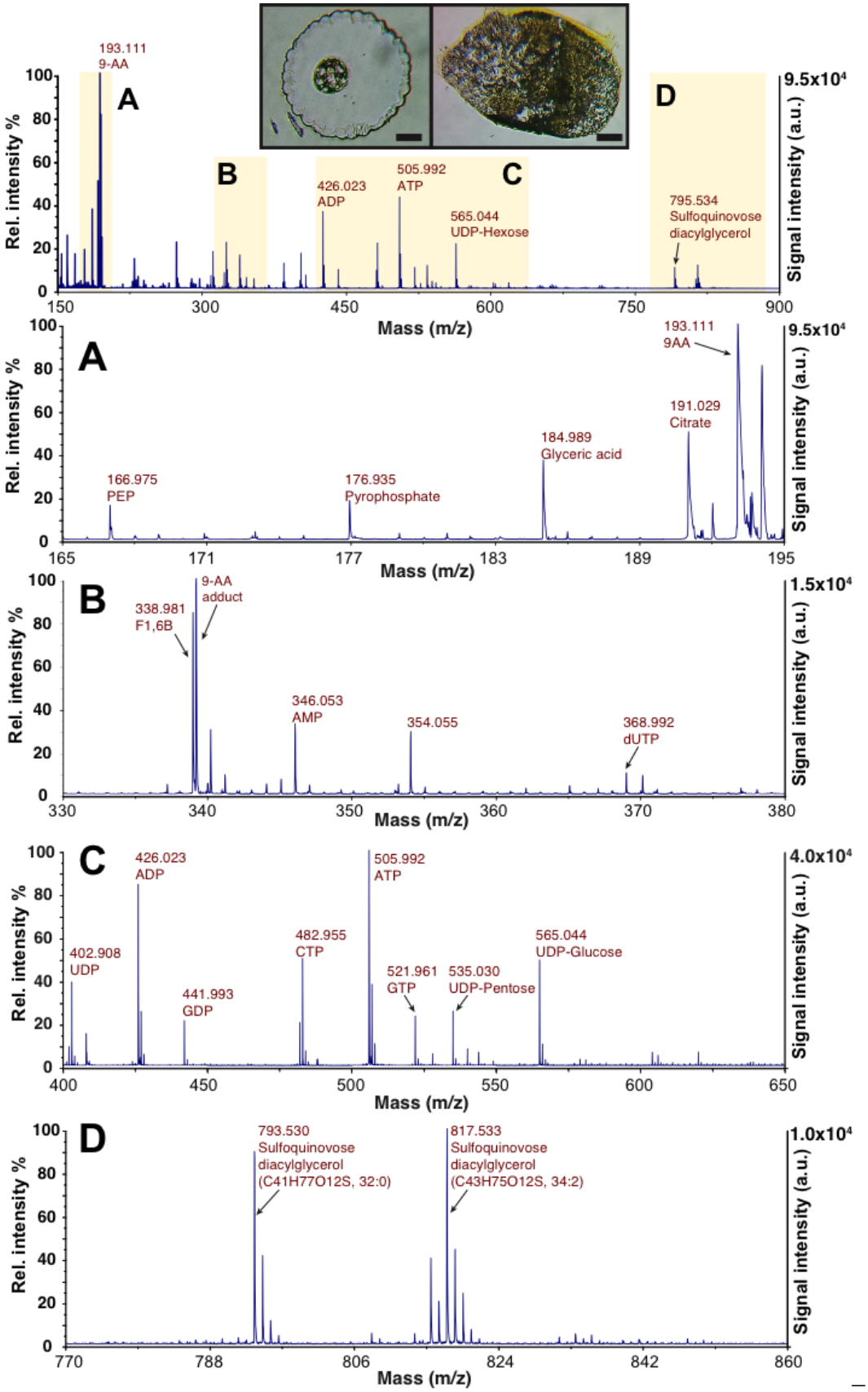


**Fig. S-6** Mass spectrum of a single *H. pluvialis* cell. The two images show the cell held in a well of the MAMS chip before (left) and after (right) application of MALDI matrix. The scale bar corresponds to 20 µm. The spectra below represent segments of the top spectrum.

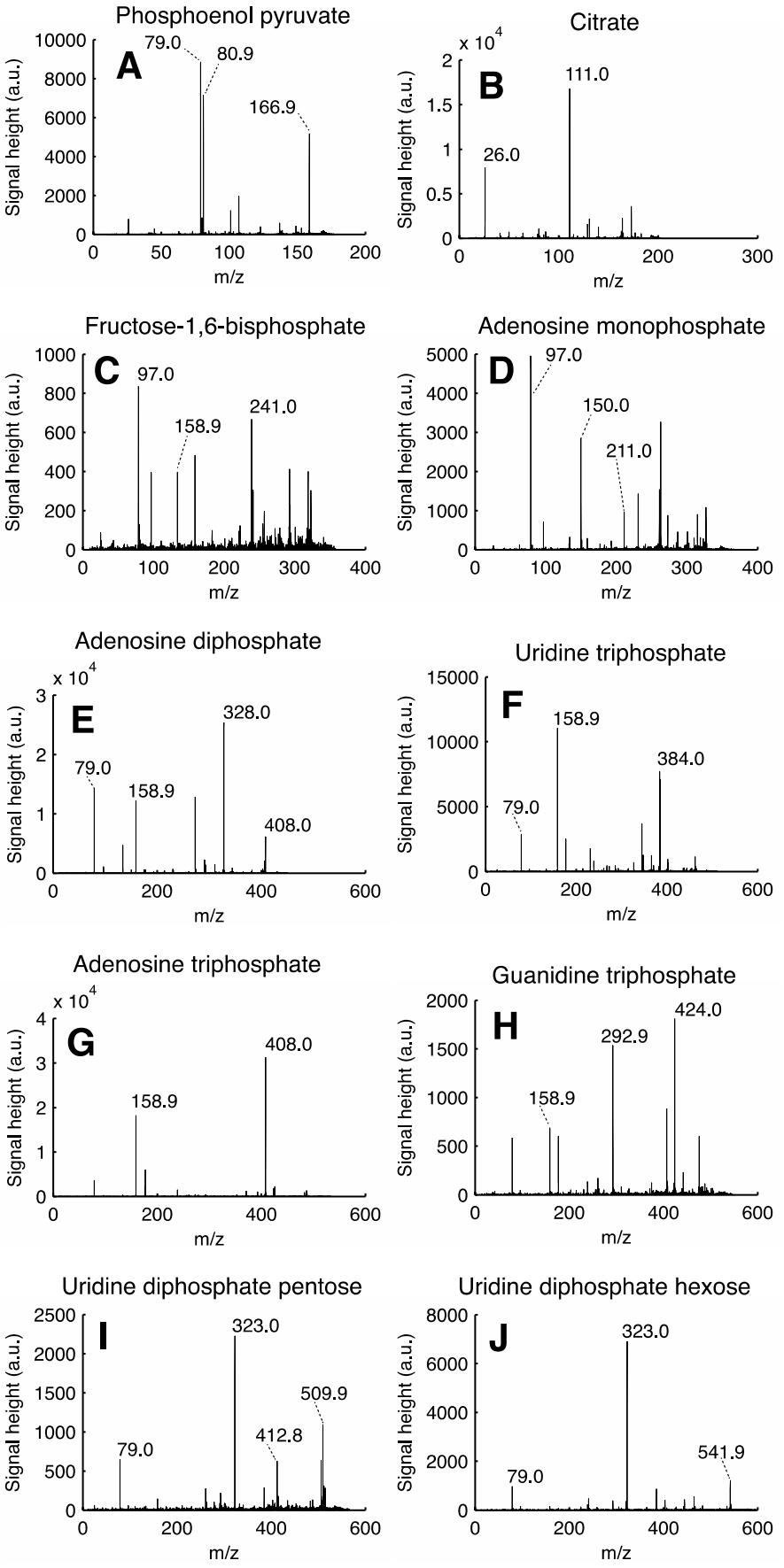

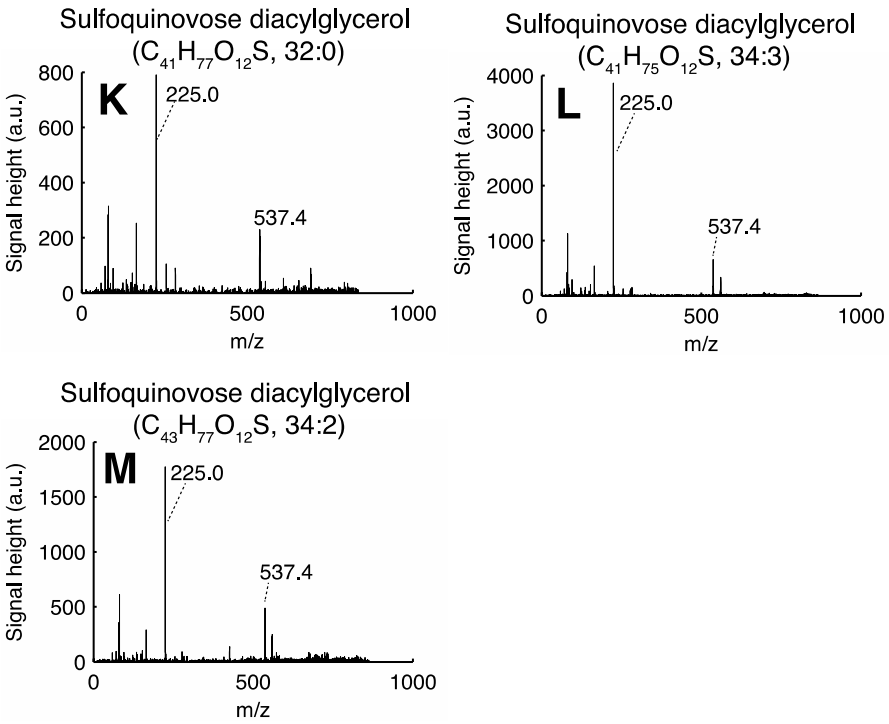


**Fig. S-7** MS/MS spectra of all compounds in **table S-1**. The measurement was performed on the population level of *H. pluvialis* cells and using a stainless steel MALDI plate. The chemical assignment of the compounds in **table S-1** (except for the sulfoquinovose diacylglycerols, **S-7K, L** and **M**) were verified by comparison to commercially available standards (the MS/MS spectra can be downloaded from the MetaboLight online repository, **www.ebi.ac.uk/metabolights**, under the study identifier MTBLS29). The sulfoquinovose diacylglycerols (**S-7K, L** and **M**) were identified by the characteristic sulfoquinovosyl ion of 225.0 m/z.[2]

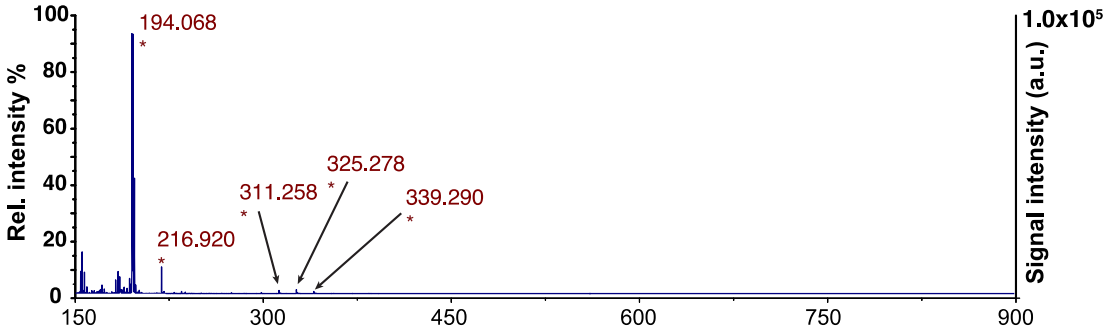


**Fig. S-8** MALDI spectrum of a filtered lysate of cysts of *H. pluvialis*.

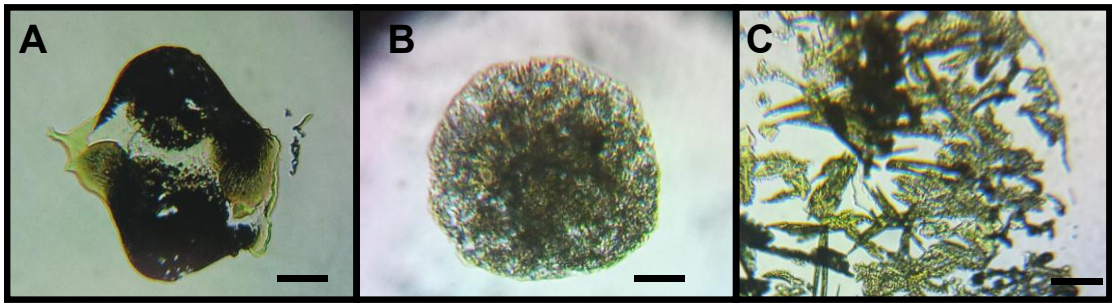


**Fig. S-9** Crystallization patterns of 9-aminoacridine at a concentration of 2 mg $mL^{-1}$ in different solvent compositions on a microarray for mass spectrometry. (A) acetone, (B) acetone/ water 9/1 (v/v), (C) acetone/ water 8/2 (v/v).

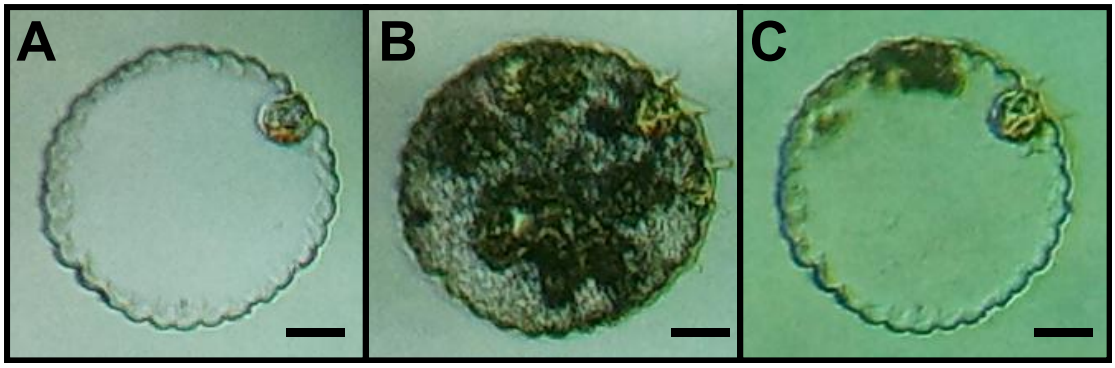


**Fig. S-10** Images of a cell on MAMS chip before (A) and after matrix deposition (B). Image in (C) shows the cell after the MALDI-MS analysis.

## References

1 Urban, P. L., Schmid, T., Amantonico, A. & Zenobi, R. Multidimensional Analysis of Single Algal Cells by Integrating Microspectroscopy with Mass Spectrometry. *Anal Chem*, doi:10.1021/ac102702m (2011).

2 He, H., Rodgers, R. P., Marshall, A. G. & Hsu, C. S. Algae Polar Lipids Characterized by Online Liquid Chromatography Coupled with Hybrid Linear Quadrupole Ion Trap/Fourier Transform Ion Cyclotron Resonance Mass Spectrometry. *Energ Fuel* **25**, 4770-4775, doi:Doi 10.1021/Ef201061j (2011).